Y/DQ-83

Photon Extremity Absorbed Dose and Kerma Conversion Coefficients for Calibration

K. G. Veinot
Y-12 National Security Complex
P.O. Box 2009, M.S. 8105
Oak Ridge, TN
and
N. E. Hertel
George W. Woodruff School of Mechanical Engineering
Georgia Institute of Technology
Atlanta, GA

2007

Note

PHOTON EXTREMITY ABSORBED DOSE AND KERMA CONVERSION COEFFICIENTS FOR CALIBRATION GEOMETRIES

K. G. Veinot* and N. E. Hertel†

Abstract—**Absorbed dose and dose equivalent conversion coefficients are routinely used in personnel dosimetry programs. These conversion coefficients can be applied to particle fluences or to measured air kerma values to determine appropriate operational monitoring quantities such as the ambient dose equivalent or personal dose equivalent for a specific geometry. For personnel directly handling materials, the absorbed dose to the extremities is of concern. This work presents photon conversion coefficients for two extremity calibration geometries using finger and wrist/arm phantoms described in HPS N13.32. These conversion coefficients have been calculated as a function of photon energy in terms of the kerma and the absorbed dose using Monte Carlo techniques and the calibration geometries specified in HPS N13.32. Additionally, kerma and absorbed dose conversion coefficients for commonly used x-ray spectra and calibration source fields are presented. The kerma values calculated in this work for the x-ray spectra and calibration sources compare well to those listed in HPS N13.32. The absorbed dose values, however, differ significantly for higher energy photons because charged particle equilibrium conditions have not been satisfied for the shallow depth. Thus, the air-kerma-to-dose and exposure-to-dose conversion coefficients for ^{137}Cs and ^{60}Co listed in HPS N13.32 overestimate the absorbed dose to the extremities. Applying the conversion coefficients listed in HPS N13.32 for ^{137}Cs, for example, would result in an overestimate of absorbed dose of 62% for the finger phantom and 55% for the wrist phantom.**
Health Phys. 92(2):179–185; 2007

Key words: dose, absorbed; photons; extremities; dosimetry, personnel

INTRODUCTION

MANY U.S. Department of Energy (U.S. DOE) workers handling radioactive materials are required to wear extremity dosimeters to measure the dose equivalent to the sensitive layer of the skin, which is taken to be 0.007 cm tissue depth. The International Commission on Radiation Units and Measurements (ICRU) has defined a number of quantities for use in personnel monitoring (ICRU 1992, 1993) including the personal dose equivalent $H_p(d)$. The depth, d, is dependent on the penetrating qualities of the radiation and, in the case of weakly penetrating radiations, the depth is taken to be 0.007 cm. The ICRU further states that the calibration of dosimeters is to be performed under simplified conventional conditions on an appropriate phantom. Since the personal dose equivalent is defined on the human body, $H_p(d)$ can vary both between individuals and between locations on the individual (ICRU 1998).

For extremity monitoring at U.S. DOE facilities, the tissue depth of interest remains 0.007 cm, but the phantom used is specified in HPS N13.32 Performance Testing of Extremity Dosimeters (ANSI/HPS 1995). Specifically, for finger monitoring, HPS N13.32 defines a solid right-circular cylinder with diameter of 1.9 cm and length of at least 30 cm constructed of polymethylmethacrylate (PMMA) to be used during dosimeter calibration and testing. An arm/wrist phantom is also defined as a solid, right-circular cylinder of aluminum with diameter of 6 cm nested inside a tube of PMMA having an inner diameter of 6 cm, an outer diameter of 7.3 cm, and length of at least 30 cm (ANSI/HPS 1995). These phantom designs are similar to others defined in international standards. HPS N13.32 specifies exposure-to-absorbed dose and air-kerma-to-absorbed dose conversion factors for photons to be used based on the phantom type (arm/leg or finger), and for dosimeter calibration purposes N13.32 states that photon sources should be placed 100 cm from the nearest phantom surface (ANSI/HPS 1995). These are the irradiation geometries commonly used for dosimeter calibrations as well as for performance testing for accreditation programs such as the Department of Energy Laboratory Accreditation Program (DOELAP).

* Y-12 National Security Complex, P.O. Box 2009, M.S. 8105, Oak Ridge, TN 37831-8105; † George W. Woodruff School of Mechanical Engineering, Georgia Institute of Technology, Atlanta, GA 30332-0405.

For correspondence contact: K. G. Veinot, Y-12 National Security Complex, P.O. Box 2009, M.S. 8105, Oak Ridge, TN 37831-8105, or email at veinotkg@y12.doe.gov.

(*Manuscript accepted* 11 *August* 2006)
0017-9078/07/0

The ICRU defines the personal dose equivalent as the dose equivalent in soft tissue, at an appropriate depth, *d*, below a specified point in the body. For weakly penetrating radiation, a depth of 0.07 mm for the skin is to be used (ICRU 1993). Ferrari and Pelliccioni (1994) discussed irradiation conditions and potential errors associated with absorbed dose conversion coefficients calculated using kerma approximations. At energies above a few hundred keV, charged particle equilibrium (CPE) has not been established, particularly at shallow tissue depths, and the assumption that kerma is a reasonable approximation of absorbed dose is not valid. Additionally, Ferrari and Pelliccioni noted that the requirements of an aligned and expanded field at the phantom surface can only be achieved if the phantom is placed in a vacuum as air will lead to scattering of the photons and the presence of secondary electrons. Kim and Kim expanded on the work of Ferrari and Pelliccioni by calculating absorbed doses in the ICRU slab phantom (Kim and Kim 1999). In both works, the absorbed doses at various tissue depths were calculated using Monte Carlo transport codes to tally the energy deposition of secondary electrons produced by the photons.

In this work photon absorbed dose conversion coefficients have been calculated for the N13.32 arm and finger phantoms under two conditions. The first condition was with the phantoms placed in a vacuum and the second condition with the phantoms modeled in air and the source positioned 100 cm from the front face of each phantom. Each of these calculations was performed for specific photon energies. Additionally, common x-ray source and calibration source energies were investigated for the case of the phantoms surrounded by air.

MATERIALS AND METHODS

Photon dose conversion coefficients

Photon dose equivalent conversion coefficients were calculated using the Monte Carlo transport code MCNP version 4-C (Briesmeister 2000). For each calculation two tallies were recorded: the energy deposition (F6 tally in MCNP), which is analogous to kerma; and a modified pulse-height tally of the photons and secondary electrons (*F8 tally in MCNP) produced by the incident photons. The pulse height tally is a measure of the energy imparted within a tally volume, and the tally total accounts for energy lost when photons or electrons leave the tally volume (these losses are subtracted from the pulse height tally). This tally, therefore, is an absorbed dose tally. For all calculations the MCNP error for each tally reported herein was less than 5%, and the quality factor for electrons and photons was assumed to be unity at all energies.

Tallies were performed at a depth of 0.007 cm within the finger and arm extremity phantom described in HPS N13.32, although for these calculations the phantom was assumed to be ICRU tissue substitute rather than PMMA since absorbed doses in tissue are of interest. The model used a circular disk source of 15 cm radius to irradiate the phantom with a parallel broad beam perpendicular to the phantom axis. This source radius was chosen so as to ensure the entire phantom was irradiated and the source particles were sampled uniformly across the surface of the disk source. The parallel broad beam geometry was used in an attempt to replicate an expanded and aligned field. The space between the source and phantom was treated as a vacuum for the first set of calculations. The second set of calculations surrounded the phantom with a 200-cm-radius air sphere and the source disk was placed 100 cm from the front phantom surface. For the finger phantom the tally volume was a cylindrical cross section with 0.942 cm inner radius, 0.944 cm outer radius, 1 cm height, and outer arc-length of 0.2004 cm. The arm phantom tally volume was modeled with a height of 6 cm, outer radius of 3.644, inner radius of 3.642, and the outer arc-length increased to 2.0260 cm. The finger and wrist phantom models are shown in Fig. 1 and Fig. 2, respectively. These geometries replicate those encountered when performing dosimeter calibrations.

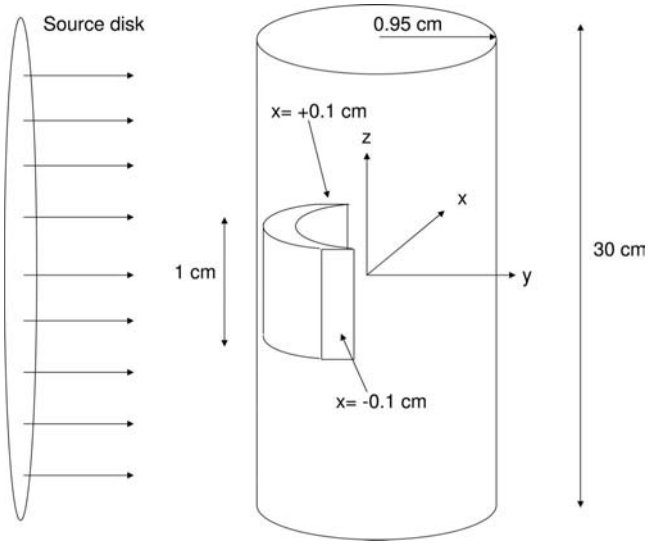

Fig. 1. Extremity finger phantom model (not to scale). The tally volume is centered at a depth of 0.007 cm from the front face of the phantom opposing the circular disk source. The radius of the inner tally volume cylinder section is 0.942 cm and the radius of the outer cylindrical section is 0.944 cm. For the calculations that included air the entire geometry was enclosed within a 200-cm-radius sphere of air.

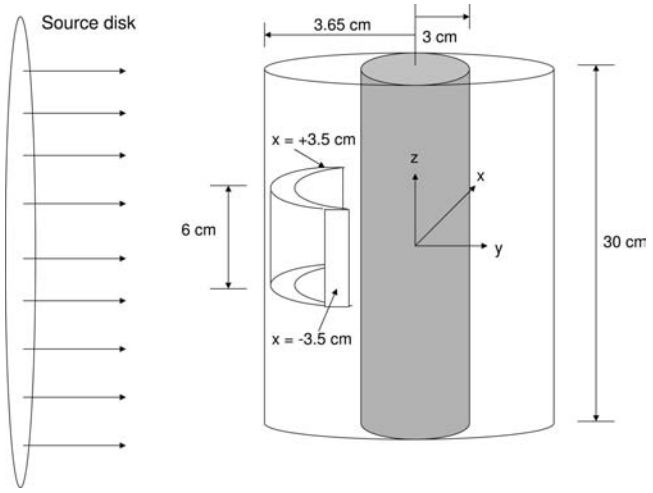

Fig. 2. Extremity arm phantom model (not to scale). The tally volume is centered at a depth of 0.007 cm from the front face of the phantom opposing the circular disk source. The radius of the inner tally volume cylinder section is 3.642 cm and the radius of the outer cylindrical section is 3.644 cm. For the calculations that included air the entire geometry was enclosed within a 200-cm-radius sphere of air.

X-ray and calibration source dose conversion coefficients

Since dosimeters are calibrated using x-ray beams and sources, calculations for these photon energies were performed. The x-ray spectra used included M-30 (average energy of 0.021 MeV), M-60 (average energy of 0.035 MeV), M-100 (average energy of 0.053 MeV), M-150 (average energy of 0.074 MeV), and H-150 (average energy of 0.119 MeV). Calibration sources used included ^{137}Cs (energy of 0.662 MeV) and ^{60}Co (average energy of 1.25 MeV). Calculations for these sources were performed using the same model described earlier. The x-ray spectra were taken from HPS N13.11 (ANSI/HPS 1993) and the models included air surrounding the phantoms. The x-ray spectra are shown in Fig. 3. The entire irradiation geometry (source disk and phantom) was modeled within a 200-cm-radius sphere filled with air at a density of 1.2929×10^{-3} g cm^{-3} with the phantom centered at the origin.

Air kerma conversion coefficients

Photon dose conversion coefficients are commonly listed in terms of the air kerma (K_a) that would be produced from the same photon energy fluence. Air kerma conversion coefficients were calculated for both single photon energies as well as for the x-ray spectra and calibration source energies. These calculations were performed using MCNP by tallying the kerma (F6 tally) from photons within a rectangular solid air volume with height, width, and depth of 1 cm.

For all calculations, MCNP normalizes the output to a per source-particle tally. To convert this result to fluence per unit area, the MCNP output was multiplied by the area of the source disk (706.86 cm^2).

RESULTS

The calculated air kerma conversion coefficients are shown in Fig. 4 and are compared to those listed in ICRP

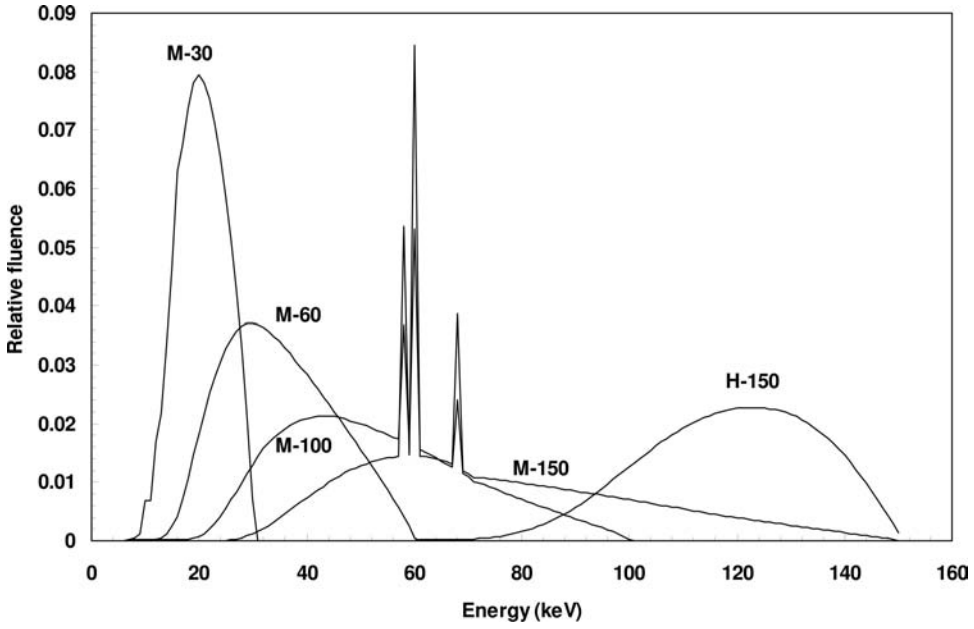

Fig. 3. X-ray photon spectra taken from HPS N13.11 (1993). Each spectrum has been normalized to fluence per photon output.

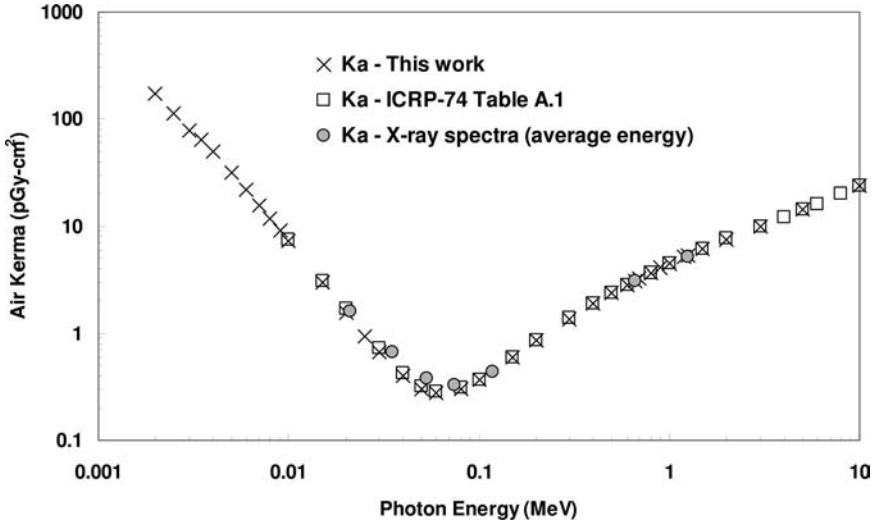

Fig. 4. Air kerma conversion coefficients for photons. X-ray air kerma values are shown by average photon energy of the x-ray spectrum.

74 (ICRP 1996). Also shown are the air kerma conversion coefficients for the x-ray and calibration source photons. X-ray air kerma conversion coefficients are plotted based on their average photon energies.

The calculated photon dose equivalent conversion coefficients for the finger and arm phantoms are listed in Table 1 and Table 2, respectively. The conversion coefficients are shown in Fig. 5 for the finger phantom and in Fig. 6 for the arm phantom as the ratio of absorbed dose conversion coefficient to air kerma. Also shown in Figs. 5 and 6 are the kerma values calculated in this work for the case of vacuum between source and phantom. The

Table 1. Calculated photon dose equivalent conversion coefficients for the finger phantom.

Photon energy (MeV)	Air kerma (pGy cm^{-2})	Vacuum kerma (pGy cm^{-2})	Vacuum absorbed dose (pGy cm^{-2})	100 cm air kerma (pGy cm^{-2})	100 cm air absorbed dose (pGy cm^{-2})
0.002	171.5	1.44	1.44	—	—
0.003	78.7	16.3	16.3	—	—
0.004	49.3	23.2	23.2	—	—
0.005	31.6	21.0	21.0	0.12	0.12
0.006	21.6	16.9	17.0	0.87	0.85
0.007	15.6	13.2	13.4	2.09	2.08
0.008	11.7	10.4	10.6	3.06	3.01
0.01	7.25	6.75	6.75	3.63	3.61
0.015	2.98	2.92	2.90	2.42	2.42
0.02	1.58	1.60	1.58	1.47	1.49
0.03	0.67	0.71	0.69	0.68	0.70
0.04	0.40	0.44	0.42	0.43	0.43
0.05	0.31	0.34	0.35	0.34	0.33
0.06	0.28	0.32	0.33	0.31	0.31
0.08	0.30	0.35	0.35	0.35	0.35
0.1	0.37	0.43	0.43	0.43	0.41
0.15	0.60	0.70	0.70	0.69	0.68
0.2	0.85	0.99	0.97	0.97	0.93
0.3	1.38	1.57	1.07	1.55	1.50
0.5	2.37	2.68	1.02	2.65	2.09
0.6	2.83	3.18	0.99	3.16	2.15
0.662	3.10	3.48	0.96	3.45	2.19
0.8	3.69	4.13	0.90	4.10	2.04
1	4.46	4.98	0.87	4.95	1.94
1.25	5.30	5.91	0.81	5.88	1.84
2	7.52	8.35	0.65	8.32	1.53
5	14.1	15.5	0.33	15.4	1.02
10	24.0	25.7	0.17	25.7	0.93

Table 2. Calculated photon dose equivalent conversion coefficients for the arm phantom.

Photon energy (MeV)	Air kerma (pGy cm^{-2})	Vacuum kerma (pGy cm^{-2})	Vacuum absorbed dose (pGy cm^{-2})	100 cm air kerma (pGy cm^{-2})	100 cm air absorbed dose (pGy cm^{-2})
0.002	171.5	1.42	1.42	—	—
0.003	78.7	16.0	15.9	—	—
0.004	49.3	22.9	22.9	—	—
0.005	31.6	20.8	20.9	0.13	0.13
0.006	21.6	16.8	16.7	0.92	0.90
0.007	15.6	13.2	13.1	2.17	2.16
0.008	11.7	10.4	10.4	3.13	3.09
0.01	7.25	6.76	6.75	3.66	3.64
0.015	2.98	2.93	2.89	2.43	2.39
0.02	1.58	1.61	1.53	1.48	1.39
0.03	0.67	0.72	0.73	0.70	0.70
0.04	0.40	0.46	0.47	0.45	0.44
0.05	0.31	0.37	0.37	0.36	0.37
0.06	0.28	0.35	0.35	0.35	0.35
0.08	0.30	0.40	0.40	0.40	0.40
0.1	0.37	0.50	0.49	0.49	0.49
0.15	0.60	0.79	0.80	0.78	0.79
0.2	0.85	1.10	1.08	1.09	1.08
0.3	1.38	1.72	1.20	1.70	1.67
0.5	2.37	2.84	1.18	2.81	2.23
0.6	2.83	3.35	1.19	3.32	2.29
0.662	3.10	3.65	1.18	3.62	2.28
0.8	3.69	4.29	1.10	4.26	2.23
1	4.46	5.14	1.07	5.11	2.16
1.25	5.30	6.06	1.04	6.03	2.06
2	7.52	8.49	0.91	8.45	1.72
5	14.1	15.6	0.78	15.5	1.49
10	24.0	25.9	0.64	25.8	1.39

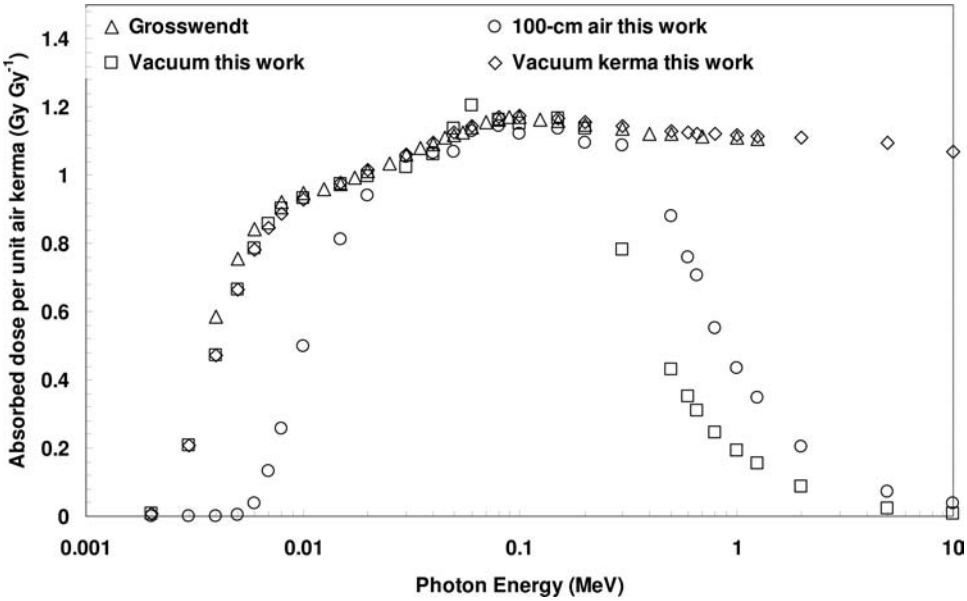

Fig. 5. Photon conversion coefficients for the finger phantom. Results are compared to those reported by Grosswendt for the "rod" phantom which has identical dimensions as those for the finger phantom used in this work. Vacuum indicates the region between the source and phantom was treated as a void. Also shown is the kerma calculated in this work assuming a vacuum between the source disk and phantom.

data in Figs. 5 and 6 are compared to values reported by Grosswendt (1995), which were determined by calculating the collisional kerma in the arm and finger phantoms within a vacuum. Table 3 lists the absorbed dose conversion coefficients (calculated with 100 cm of air between the source and phantom) and the air kerma conversion coefficients for the calibration sources and x-ray spectra for each phantom. Table 4 provides a comparison between the air-kerma-to-absorbed dose conversion coefficients listed in HPS N13.32 and those

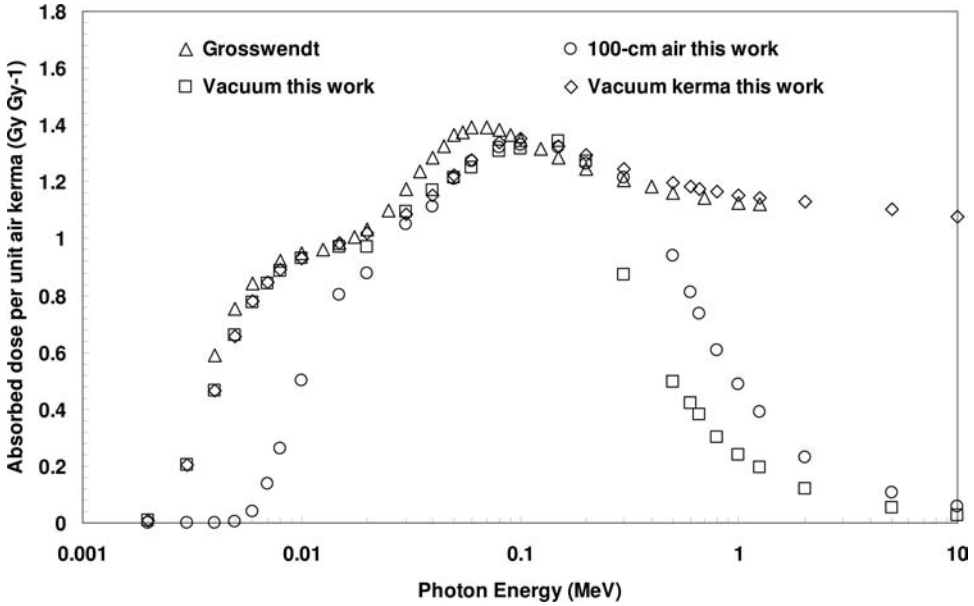

Fig. 6. Photon conversion coefficients for the arm phantom. Results are compared to those reported by Grosswendt for the "pillar" phantom which has identical dimensions as those for the arm phantom used in this work. Vacuum indicates the region between the source and phantom was treated as a void. Also shown is the kerma calculated in this work assuming a vacuum between the source disk and phantom.

Table 3. Absorbed dose conversion coefficients and air kerma conversion coefficients for the calibration sources and x-ray spectra for each phantom.

			Finger		Wrist	
Source or x-ray beam code	Average photon energy (MeV)	Air kerma (pGy cm^{-2})	100 cm air kerma (pGy cm^{-2})	100 cm air absorbed dose (pGy cm^{-2})	100 cm air kerma (pGy cm^{-2})	100 cm air absorbed dose (pGy cm^{-2})
M-30	0.021	1.59	1.60	1.64	1.61	1.69
M-60	0.035	0.66	0.69	0.72	0.71	0.74
M-100	0.053	0.38	0.42	0.42	0.45	0.45
M-150	0.074	0.33	0.38	0.38	0.42	0.42
H-150	0.119	0.44	0.52	0.52	0.59	0.60
^{137}Cs	0.662	3.05	3.48	2.11	3.64	2.29
^{60}Co	1.25	5.20	5.88	1.87	6.03	2.07

Table 4. Comparison between the air-kerma-to-absorbed dose conversion coefficients.

Source or x-ray beam code	Finger phantom D/Ka (Gy Gy^{-1})		Arm phantom D/Ka (Gy Gy^{-1})	
	HPS N13.32	This work	HPS N13.32	This work
M-30	1.08	1.03	1.13	1.06
M-60	1.12	1.08	1.19	1.12
M-100	1.13	1.11	1.26	1.19
M-150	1.15	1.15	1.3	1.28
H-150	1.16	1.17	1.29	1.36
^{137}Cs	1.12	0.69	1.16	0.75
^{60}Co	1.12	0.36	1.14	0.40

calculated in this work for common x-ray spectra and calibration sources.

DISCUSSION

The extremity phantoms are defined in HPS N13.32 but the method of calculation is not. Thus, the parameters used to tally energy deposition may vary depending on certain variables. For the calculations in this work the tally volumes were relatively small and thin. Varying this tally volume (especially the thickness of the tally volume) will likely change the values presented here, so additional calculations are needed to determine the effects of these changes. Although the phantoms defined in

HPS N13.32 are constructed of PMMA, the use of ICRU tissue substitute seems more appropriate.

Absorbed dose calculations, especially when calibrating dosimeters, are commonly performed by measuring the air kerma (or the exposure) at a point and applying the conversion coefficient for the radiation field. From Fig. 5 and Fig. 6 it is seen that care must be taken for photon energies greater than 300 keV as the tissue kerma begins to overestimate the absorbed dose in this region. This overestimation is caused by a lack of charged particle equilibrium at the depth of 0.007 cm in tissue. Below 20 keV the effect of including 100 cm of air between the source and the phantom (as defined in N13.32) is evident in Figs. 5 and 6. Secondary electrons produced in air between the source disk and phantom allow for CPE conditions to be met within the tally volume for higher photon energies. This can be seen clearly in Fig. 5 where the absorbed dose in the vacuum case begins to differ significantly from the case where air is included above 300 keV. A similar effect is seen in Fig. 6 for the arm phantom. In general, the kerma calculations agree very well with those listed by Grosswendt. Minor differences between the values determined here and in those reported by Grosswendt are likely due to different modeling parameters and tally techniques. The use of a disk source in this work seems appropriate since the intent was to replicate as closely as possible the conditions of an expanded and aligned field according to ICRU recommendations, although the aligned field requirements are invalidated in the case where air is included since photons will be scattered as they traverse the region between the source and the phantom.

For the case of a calibration source placed 100 cm from the phantom, the field is not diverging rapidly at the phantom and the conversion coefficients should be very similar to those derived using the disk source. Some internal scatter from the encapsulation of ^{137}Cs and ^{60}Co sources would be expected causing the photon spectra to soften slightly, although this softening would not likely significantly change the results determined here using the planar disk source geometry. A test case modeled using the wrist phantom and a right cylindrical ^{137}Cs source encapsulated with 0.1 cm of stainless steel confirmed this. For facilities that calibrate their dosimeters using either ^{137}Cs or ^{60}Co, the air-kerma-to-absorbed dose conversion coefficient differs significantly from the tissue kerma, and these differences should be considered. For ^{137}Cs, the dose-to-air kerma values listed in HPS N13.32 overestimate the absorbed dose by 62% for the finger phantom and by 55% for the arm phantom. The N13.32 values for ^{60}Co overestimate the absorbed dose by 311% for the finger phantom and 285% for the wrist phantom.

The conversion coefficients calculated here further demonstrate the need to consider secondary electron production when deriving absorbed dose conversion coefficients for photons. Future work will consider the effects of variations in the tally volume sizes and shapes, angular dependences, the adequacy of aluminum as a bone substitute, and the effects of including ICRU compact bone in the finger phantom.

REFERENCES

American National Standards Institute and the Health Physics Society. Personnel dosimetry performance—criteria for testing. McLean, VA: Health Physics Society; ANSI/HPS N13.11; 1993.

American National Standards Institute and the Health Physics Society. Performance testing of extremity dosimeters. McLean, VA: Health Physics Society; ANSI/HPS N13.32; 1995.

Briesmeister J. MCNP—a general Monte Carlo N-particle transport code. Version 4C. Los Alamos, NM: Transport Methods Group, Los Alamos National Laboratory; LA-13709-M; 2000.

Ferrari A, Pelliccioni M. On the conversion coefficients from fluence to ambient dose equivalent. Radiat Prot Dosim 51:251–255; 1994.

Grosswendt B. Angular dependence factors and air kerma to dose equivalent conversion coefficients for cylindrical phantoms irradiated by plane-parallel extended monoenergetic photon beams. Radiat Prot Dosim 59:165–179; 1995.

International Commission on Radiation Units and Measurements. Measurement of dose equivalents from external photon and electron radiations. Bethesda, MD: ICRU; Publication 47; 1992.

International Commission on Radiation Units and Measurements. Quantities and units in radiation protection dosimetry. Bethesda, MD: ICRU; Publication 51; 1993.

International Commission on Radiation Units and Measurements. Conversion coefficients for use in radiological protection against external radiation. Bethesda, MD: ICRU; Publication 57; 1998.

International Commission on Radiological Protection. Conversion coefficients for use in radiological protection against external radiation. Oxford: Pergamon Press; ICRP Publication 74; 1996.

Kim JO, Kim JK. Dose equivalent per unit fluence near the surface of the ICRU phantom by including the secondary electron transport for photons. Radiat Prot Dosim 83:211–219; 1999.

■ ■